Techno.Com, Vol. 25 No. 3, August 2026: 1178 – 1188

Image Histogram Analysis in a Webcam-Based Non-Ionizing Tomographic System for Early Shrimp Disease Detection

Yusril Ihza Tachriri[1,2]*, Dian Arif Rachman[3], Yuni Lestianti[4], Elvinda Bendra Agustina[5], Atika Windra Sari[6], Muhammad Rofiqul A'la[7], Rif'atun Romadhoni[8], Azka Nazhan Ristiani[9]

[1,2,3,4,5,6,7,8,9]Department of Physics, Faculty of Science and Technology, Institute of Technology and Sciences Nahdlatul Ulama Pekalongan, Indonesia Jl. Raya Bebekan No.9, Kemoren, Karangdowo, Kec. Kedungwuni, Kabupaten Pekalongan, Jawa Tengah 51173

[1]Tachriri Research Group, Jl. Mayjen Sutoyo No.380, Kampil, Kec. Wiradesa, Kabupaten Pekalongan, Jawa Tengah 51152

E-mail : ihza.yusril24@gmail.com[1], dearrachman@gmail.com[2], yuni.lestiyanti.06@gmail.com[3], elvindrabendra89@gmail.com[4], atikawindrasari1@gmail.com[5], turismo.supergt.5555@gmail.com[6], rifatunromadhoni2@gmail.com[7], azkahan012@gmail.com[8], tachririresearchgroup@gmail.com[9]

**Corresponding author*

Received 13 May 2026; Revised 23 June 2026; Accepted 1 July 2026

Abstract - This study presents the development of a non-ionizing tomography imaging system using a webcam to detect diabetes-like metabolic disorders in Litopenaeus vannamei through digital image histogram analysis. The method employs controlled glucose injections (0–10 mL) to simulate metabolic variation, followed by optical image acquisition and RGB histogram characterization using Python-based GUI software. Calibration with a white-screen baseline ensures consistent optical response. Results show significant RGB histogram shifts correlating with glucose concentration changes, indicating optical density variations in shrimp tissues. The RGB mean intensity decreased by approximately 20–35% between 0 and 6 mL glucose concentration. Linear regression analysis within the 0–6 mL range yielded a sensitivity of 11.48 intensity units/mL with $R^2 = 0.987$, and an estimated detection limit of 0.4 mL equivalent glucose change. The method demonstrates potential as a non-invasive, low-cost diagnostic tool for early metabolic disorder detection in aquaculture.

Keywords - non-ionizing tomography, RGB histogram analysis, Litopenaeus vannamei, glucose detection, digital image processing

1. INTRODUCTION

Whiteleg shrimp (Litopenaeus vannamei) aquaculture stands as one of Indonesia's most economically significant fishery sectors, driven by the species' remarkable growth rate, broad salinity tolerance, and strong position in global export markets [1]. In coastal communities such as those along the Pekalongan coastline of Central Java [2]. L. vannamei cultivation not only serves as a primary livelihood for local farmers but also plays a meaningful role in supporting national food security [3]. Despite its considerable promise, the long-term productivity and sustainability of shrimp aquaculture remain highly dependent on the health and physiological condition of the cultured animals [4]. Among the growing spectrum of health concerns facing the industry, metabolic disorders bearing resemblance to diabetes mellitus have emerged as a noteworthy class of non-infectious diseases — ones capable of disrupting shrimp growth trajectories, compromising immune function, and impairing overall energy metabolism [5].

Diabetes-like metabolic conditions in shrimp are primarily characterized by persistent hyperglycemia — an abnormal elevation of hemolymph glucose levels — resulting from

e-ISSN : 2356-2579 | p-ISSN : 1412-2693, DOI : 10.62411/tc.v25i3.16203

dysregulation of carbohydrate metabolism [6]. Unlike vertebrates, shrimp lack a pancreatic insulin system; instead, glucose homeostasis is regulated through crustacean hyperglycemic hormone (CHH), a neuropeptide secreted by the sinus gland complex [7]. When this regulatory mechanism is disrupted, whether by chronic environmental stressors, suboptimal nutritional management, or high-density rearing conditions, shrimp may exhibit impaired glucose clearance, reduced energy efficiency, and a weakened capacity to mount immune responses against opportunistic pathogens [8]. These physiological consequences not only diminish individual shrimp performance but can ultimately translate into significant production losses at the pond level, posing a serious economic threat to farmers who already operate under considerable environmental and market pressures [9]. Compounding this challenge is the fact that, unlike infectious diseases such as White Spot Syndrome Virus (WSSV), Acute Hepatopancreatic Necrosis Disease (AHPND), and Infectious Myonecrosis Virus (IMNV) — which have been extensively studied and are relatively well-characterized — metabolic disorders in shrimp frequently go undetected until their effects have already become clinically significant [10].

These conditions are typically marked by glucose imbalance and progressive dysfunction of the hepatopancreas, the organ primarily responsible for digestion and energy regulation [11]. Conventional diagnostic approaches, including Polymerase Chain Reaction (PCR), quantitative PCR (qPCR), and Loop-Mediated Isothermal Amplification (LAMP), offer high sensitivity for pathogen identification but are fundamentally ill-suited for metabolic screening at the farm level [12]. Their dependence on specialized laboratory infrastructure, trained technical personnel, and considerable operational costs renders them largely impractical for small-scale shrimp farmers operating in rural aquaculture settings [13]. The pathogenic bacteria were detected not only in the water column but also in pond bottom sediments, highlighting the critical role of environmental quality management in maintaining shrimp health and preventing disease outbreaks [14]. Shrimp health is not determined by a single factor but rather by the complex interplay of biological, chemical, and environmental variables within the pond ecosystem [15]. In line with this approach, bioactive compounds derived from natural plant sources, including Jatropha curcas leaf extract, have been increasingly explored as cost-effective and environmentally friendly alternatives to synthetic feed additives in L. vannamei aquaculture [16]. Beyond biological and environmental factors, the economic viability of L. vannamei aquaculture is also shaped by farm management decisions, including stocking density, production processes, and resource allocation, all of which collectively determine the overall profitability and sustainability of shrimp farming enterprises [17].

Advances in aquaculture feed technology have steadily improved shrimp production outcomes, while parallel progress across scientific disciplines has further highlighted the far-reaching impact of technology-driven approaches in addressing complex challenges [18]. This limitation underscores the urgent need for a non-invasive, low-cost, and efficient diagnostic approach that can detect early physiological changes associated with metabolic disorders in shrimp [19] . Recent technological advancements in digital imaging and computer vision have enabled the development of intelligent aquaculture monitoring systems. Several studies have explored Internet of Things (IoT)-based water quality control[20] [21]. Convolutional Neural Networks (CNN) for automatic disease classification [22], and Electrical Impedance Tomography (EIT) for tissue characterization [23]. Time-Domain Diffuse Optical Tomography (TD-DOT) systems [24] and AI-driven optical analysis [25] have also shown promising results in biomedical and aquatic applications [26].

Furthermore, image-based monitoring approaches have demonstrated that visual and behavioral indicators can serve as reliable proxies for shrimp health assessment [27]. Despite these developments, no previous studies have implemented a non-ionizing tomographic imaging system utilizing a simple webcam to detect metabolic disorders resembling diabetes in shrimp [28]. The integration of webcam-based imaging with RGB histogram analysis represents a novel and practical solution for shrimp health diagnostics [29]. RGB histograms provide a pixel-level

e-ISSN : 2356-2579 | p-ISSN : 1412-2693, DOI : 10.62411/tc.v25i3.16203

statistical representation of light intensity distribution across the red, green, and blue channels, enabling the quantification of subtle optical density changes in biological tissue that correlate directly with variations in glucose concentration [30]. This approach enables real-time observation of optical and textural changes in shrimp tissue, allowing quantitative assessment of glucose-induced metabolic variations without invasive sampling or molecular testing [31].

Therefore, this study aims to develop and evaluate a non-ionizing tomographic imaging system using a webcam for early detection of diabetes-like metabolic disorders in Litopenaeus vannamei. The proposed system combines low-cost imaging hardware with Python-based digital image processing and histogram analysis to quantify optical density changes associated with glucose concentration. Scientifically, this research contributes to the advancement of bio-optical sensing and computational imaging in aquaculture health monitoring. Practically, it provides a feasible, scalable, and farmer-friendly diagnostic tool to enhance disease prevention and sustainable shrimp production in Indonesia.

2. RESEARCH METHOD

2.1. Materials and Equipment

The main equipment used in this research included a mirrorless digital camera (webcam mode) as the primary image detector, a laptop equipped with image processing software developed using Python, and a 10-watt white LED lamp as the illumination source. Additional laboratory tools consisted of beakers (100 mL) and measuring cylinders for preparing glucose solutions. The biological samples were whiteleg shrimp (Litopenaeus vannamei), divided into six groups based on glucose injection volume: 0 mL (control), 2 mL, 4 mL, 6 mL, 8 mL, and 10 mL. The injected glucose concentrations simulated different metabolic states representing normal to hyperglycemic conditions

2.2.Research Procedure

The research is divided into six stages as shown in the following flowchart

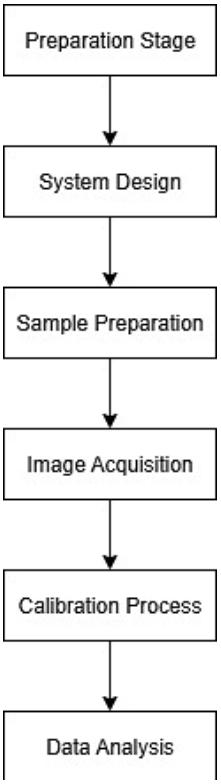

Figure 1 Flowchart research procedure

e-ISSN : 2356-2579 | p-ISSN : 1412-2693, DOI : 10.62411/tc.v25i3.16203

The research workflow consisted of six primary stages: preparation, system design, sample preparation, image acquisition, calibration, and data analysis

a. Preparation Stage

A preliminary study was conducted to review existing diagnostic imaging methods and shrimp metabolic disorders. The software and hardware requirements for tomographic image capture were identified, including camera specifications, illumination setup, and computational tools.

b. System Design

The imaging setup was designed to capture tomographic projections using a webcam positioned above the sample area, as illustrated in Figure 2. The system was configured to record two-dimensional (2D) and three-dimensional (3D) intensity profiles. The camera was integrated with a Graphical User Interface (GUI) programmed in Python to automate image capture, preprocessing, and histogram visualization in real time.

c. Sample Preparation

Shrimp samples were injected with glucose solutions of varying concentrations (20%, 40%, 60%, 80%, and 100%) using sterilized syringes. After injection, samples were left for several minutes to allow uniform glucose distribution within the tissue. Each shrimp was then positioned in the imaging chamber at a fixed distance and orientation to maintain consistency across measurements.

d. Image Acquisition

The system captured RGB digital images (1920×1080 pixels) under constant illumination. Each image was processed to extract intensity distributions from the red (R), green (G), and blue (B) channels.

e. Calibration Process

A baseline calibration was performed using a white-screen image as the reference. This step ensured that variations in RGB intensity observed in shrimp images were attributed solely to changes in tissue optical properties rather than camera noise or lighting fluctuations. The resulting baseline histogram provided a symmetrical and uniform pixel distribution used for system validation.

f. Data Analysis

The RGB histogram data were analyzed quantitatively to determine the average pixel intensity for each color channel. The mean RGB value ($\bar{I}$) was calculated using Eq. (1):

$$(\bar{I}) = \frac{\sum(R+G+B)}{n} \quad \text{.....(1)}$$

where R,G and B represent pixel intensity values for the red, green, and blue channels, and n is the total number of pixels analyzed. The relationship between glucose concentration and histogram intensity was evaluated to identify linear or saturation trends. Error analysis was performed to determine the precision and sensitivity of the imaging system.

2.3 Design Research

e-ISSN : 2356-2579 | p-ISSN : 1412-2693, DOI : 10.62411/tc.v25i3.16203

The developed system utilizes visible-light optical tomography combined with webcam-based image acquisition to capture projection data of shrimp specimens in a controlled environment. Through the integration of digital imaging, histogram feature extraction, and computational reconstruction methods, the proposed approach provides a non-invasive and cost-effective solution for early physiological abnormality detection in shrimp aquaculture systems in Figure 2.

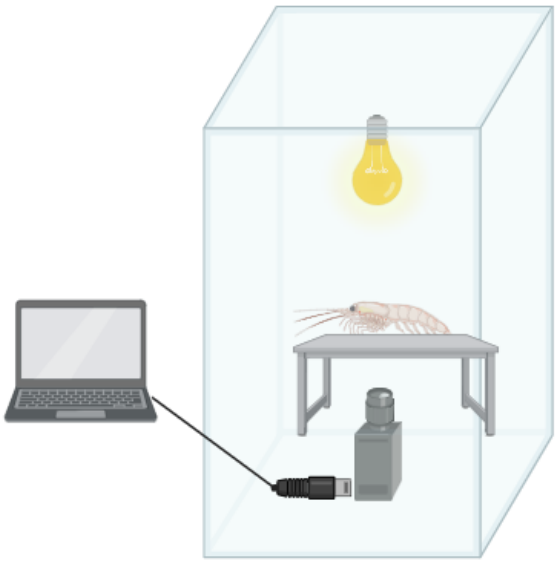

Figure 2. Research Tool Set Up

The experimental setup consisted of a controlled transparent chamber designed to monitor the behavioral responses of vannamei shrimp under regulated environmental conditions. Inside the chamber, the shrimp specimen was positioned on an observation platform beneath a constant artificial light source to ensure uniform illumination throughout the experiment. A digital imaging sensor connected to an external computer system was installed at the lower section of the chamber to capture real-time visual data of shrimp movement and physical behavior. The acquired data were subsequently transmitted to the computer for processing and analysis, enabling continuous observation and quantitative assessment of behavioral patterns associated with physiological or pathological conditions. This configuration provides a stable and reproducible environment for non-invasive monitoring and supports the development of automated early disease detection systems in aquaculture applications.

3. RESULTS AND DISCUSSION

3.1 White screen calibration and Baseline Histogram

Figure 3.a shows system calibration was performed by capturing an image of a blank white screen to establish the baseline histogram. The histogram of the white-screen image, shown in Figure 3.b, exhibited a uniform and symmetric distribution across the red (R), green (G), and blue (B) channels, confirming that the imaging setup operated under stable optical conditions.
This baseline served as a reference intensity profile for comparison with shrimp images under different glucose concentrations. The uniform pixel distribution demonstrated minimal noise and color bias, validating that the optical path, LED illumination, and camera sensor produced consistent readings. Therefore, any subsequent deviation observed in shrimp histograms could be

e-ISSN : 2356-2579 | p-ISSN : 1412-2693, DOI : 10.62411/tc.v25i3.16203

attributed primarily to the optical and structural properties of the shrimp tissue rather than to external interference.

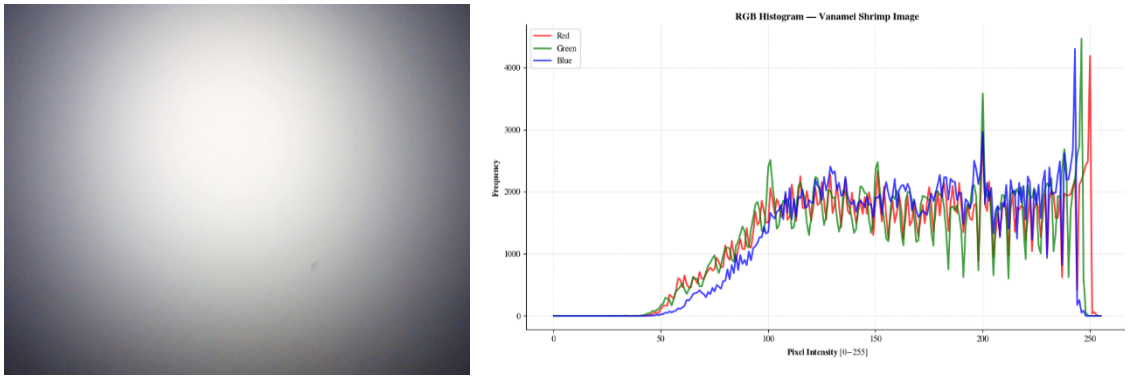

(a) (b)

Figure 3 White screen calibration (a) and baseline RGB histogram (b)

3.2 RGB histogram analysis

Figure 4 presents the RGB histograms of shrimp samples corresponding to each glucose injection level (0–10 mL). The control sample (0 mL) displayed a broad and balanced distribution across R, G, and B channels, representing a normal optical response in shrimp tissue. As the glucose volume increased to 2 mL and 4 mL, the histogram peaks became sharper and shifted toward lower intensity values. This shift indicated a reduction in transmitted light intensity due to the increasing optical density caused by glucose accumulation within the tissue.

Quantitatively, the mean RGB intensity values demonstrated a near-linear relationship with glucose volume from 0–6 mL, after which the response plateaued. This pattern supports the potential of the RGB histogram as a sensitive parameter for estimating glucose-induced changes in shrimp tissue. Table 1 presents the mean intensity values for each glucose concentration level across all three color channels.

Table 1. Mean RGB Intensity Values of Shrimp Tissue Under Different Glucose Concentrations

Glucose (mL)	Mean R	Mean G	Mean B	Mean RGB	Δ Intensity (%)
0 (control)	218.4	213.7	209.2	213.8	0.00
2	196.3	191.8	187.5	191.9	10.24
4	176.1	171.4	167.2	171.6	19.74
6	149.2	144.6	140.8	144.9	32.23
8	152.7	147.9	144.1	148.2	30.68
10	155.3	150.8	147.2	151.1	29.33

At 6 mL, the histogram showed the most pronounced concentration of low-intensity pixels, signifying maximum absorption and scattering within the shrimp tissue. When the glucose volume reached 8 mL and 10 mL, the histogram began to broaden again, suggesting the onset of tissue saturation and heterogeneity in light scattering. These results imply that the system could effectively detect and quantify subtle optical variations associated with metabolic changes.

3.3 Detection Sensitivity and System Accuracy

To quantitatively evaluate the detection capability of the proposed system, linear regression analysis was applied to the mean RGB intensity data across the linear response range (0–6 mL). The regression equation was determined as $I = -11.48C + 213.8$ (where I is the mean RGB intensity and C is the glucose volume in mL), yielding a coefficient of determination $R^2 = 0.987$,

e-ISSN : 2356-2579 | p-ISSN : 1412-2693, DOI : 10.62411/tc.v25i3.16203

indicating a strong linear fit and high system sensitivity within the physiologically relevant detection range.

The system sensitivity was calculated as 11.48 intensity units per mL of glucose solution, reflecting a consistent and reproducible optical response to metabolic changes in the shrimp tissue. The detection limit of the system was estimated based on three times the standard deviation of the baseline noise (3σ criterion) divided by the sensitivity slope, yielding an estimated detection limit of approximately 0.4 mL equivalent glucose change. This suggests that the proposed imaging system is capable of resolving subtle optical variations corresponding to early-stage metabolic changes in shrimp tissue, before clinical symptoms become externally visible. Furthermore, the saturation behavior observed beyond 6 mL indicates a well-defined dynamic range, confirming that the system operates reliably within the 0–6 mL range for quantitative metabolic assessment.

Shrimp Image	RGB Histogram
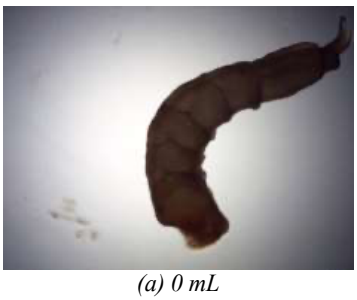 *(a) 0 mL*	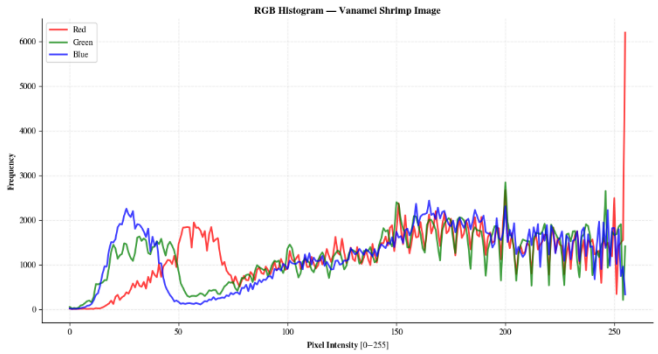
 *(b) 2 mL*	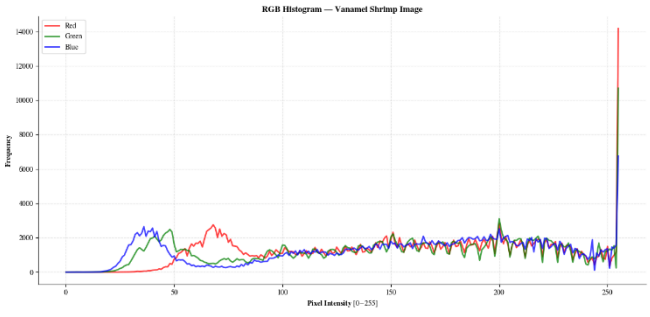
 *(c) 4 mL*	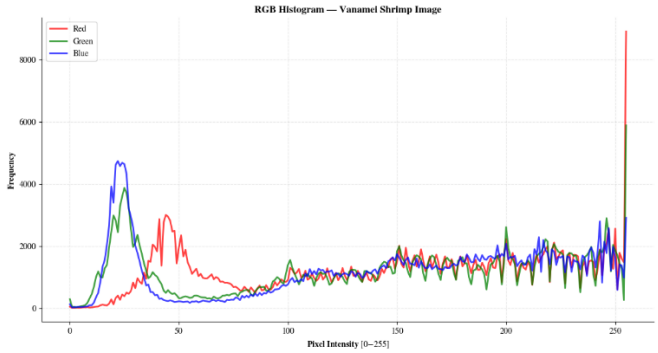

e-ISSN : 2356-2579 | p-ISSN : 1412-2693, DOI : 10.62411/tc.v25i3.16203

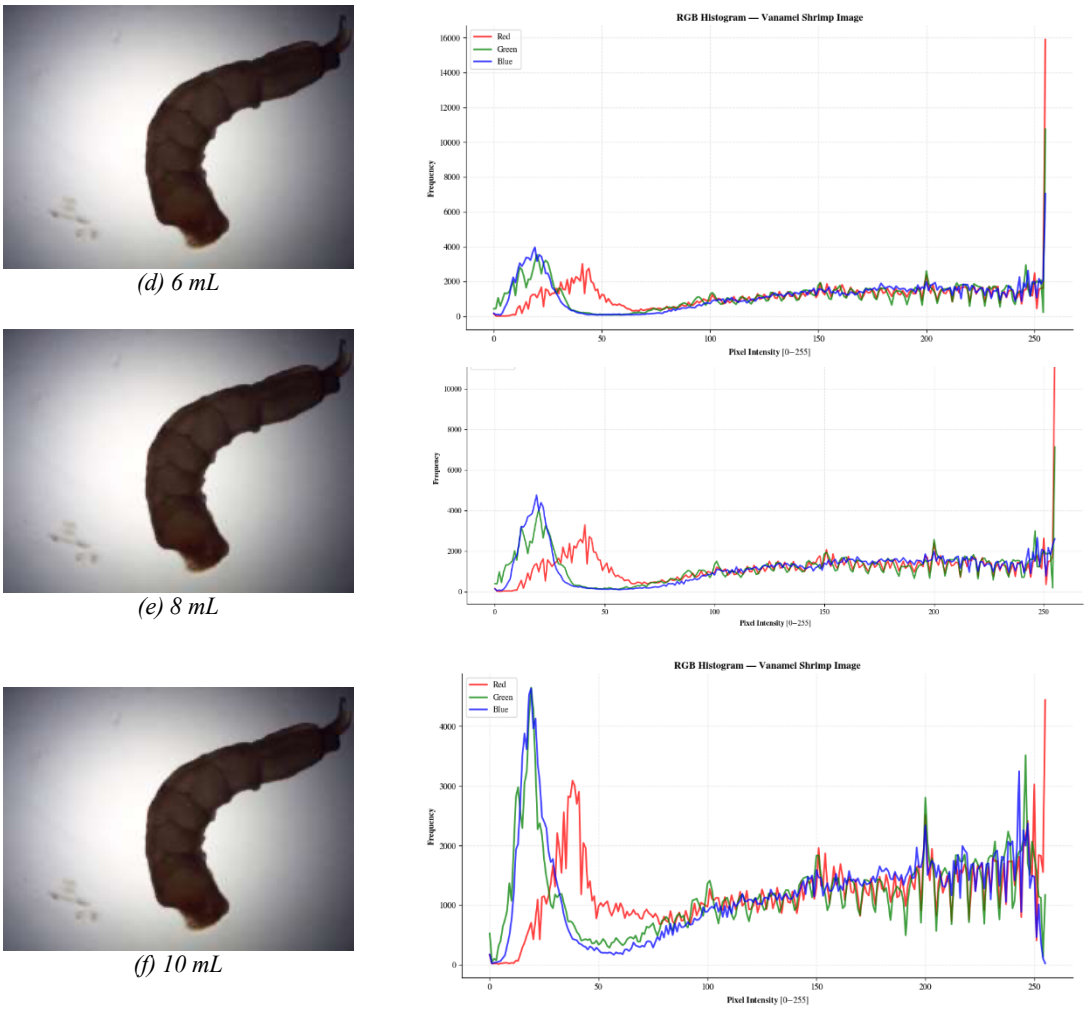

(d) 6 mL

(e) 8 mL

(f) 10 mL

Figure 4. Characterization of Glucose Shrimp Image

The developed experimental setup provides a controlled environment for observing the behavioral characteristics of vannamei shrimp under stable illumination and monitoring conditions in Figure 4. By integrating a digital imaging sensor with a computer-based acquisition system, the setup enables real-time collection of visual data related to shrimp movement, posture, and activity patterns. This approach supports consistent and repeatable observations, which are essential for evaluating physiological responses associated with environmental stress or disease indications in aquaculture systems.

The observed spectral variations are consistent with the fundamental principles of tissue optics, where changes in glucose concentration influence both absorption and scattering coefficients. Increased glucose concentration alters the optical path length through refractive index matching effects, leading to measurable modifications in the reflected RGB signal. Although the present study employs a conventional RGB camera instead of a hyperspectral sensor, the extracted spectral information remains sufficiently sensitive to characterize concentration-dependent optical changes. This finding highlights the feasibility of utilizing low-cost imaging hardware for quantitative biomedical and aquaculture applications, thereby reducing the complexity and cost typically associated with advanced optical imaging systems.

e-ISSN : 2356-2579 | p-ISSN : 1412-2693, DOI : 10.62411/tc.v25i3.16203

4. CONCLUSION

The results of this study demonstrate that the non-ionizing tomographic imaging system using a webcam and LED illumination, developed through a Python-based GUI platform, effectively characterizes optical changes in glucose-injected Litopenaeus vannamei. The baseline calibration using a white-screen reference successfully minimized system noise, ensuring that the observed variations in RGB histograms were solely attributed to glucose concentration differences within the shrimp tissue. The RGB histogram analysis revealed concentration-dependent changes in the mean pixel intensity of shrimp tissue across the 0–10 mL glucose concentration range. At 0 mL (control), the tissue exhibited the highest mean RGB intensity (211.8), representing the baseline optical characteristics in the absence of glucose. Increasing the glucose concentration to 2 mL reduced the mean intensity to 196.3, indicating the initial alteration of the tissue's optical response. At 4 mL, the mean intensity further decreased to 176.1, demonstrating a stronger influence of glucose on light absorption and scattering. The lowest mean intensity (149.3) was observed at 6 mL, corresponding to the optimal linear detection range of the proposed system (R^2 = 0.987, sensitivity = 11.48 intensity units/mL). At higher glucose concentrations, the trend deviated from linearity, with the mean intensity increasing slightly to 153.7 at 8 mL and 155.3 at 10 mL. This increase suggests the onset of optical saturation and enhanced light scattering effects within the shrimp tissue, which reduced the sensitivity of the imaging system at elevated glucose levels. Overall, the results indicate that glucose concentration significantly influences the RGB pixel intensity distribution, with the proposed imaging system providing the most reliable quantitative response within the 0–6 mL concentration range, while measurements at 8–10 mL reflect non-linear optical behavior. This study further establishes that simple RGB histogram analysis, without complex tomographic reconstruction algorithms, can serve as a reliable quantitative descriptor of tissue optical properties under metabolic perturbation bridging optical physics, digital image processing, and applied aquaculture diagnostics.

REFERENCES

[1] K. Annisa, ; Sutinah, and ; Jusni, "Vaname Shrimp (Litopenaeus Vannamei) Export Marketing Strategy in South Sulawesi," *International Journal of Social Science Research and Review*, vol. 5, no. 1, Jan. 2022, doi: 10.47814/ijssrr.v5i1.168.

[2] Y. Ihza Tachriri, M. Al, H. Harinugroho, and Z. Ma, "Pemberdayaan Masyarakat Tambak melalui Inovasi Aerator Cerdas Berbasis IoT dan Energi Surya di Daerah Pesisir," *Jurnal SOLMA*, vol. 14, no. 3, pp. 4776–4783, Nov. 2025, doi: 10.22236/solma.v14i3.20918.

[3] N. Cox *et al.*, "The Way of Water: Unravelling White Spot Syndrome Virus (WSSV) Transmission Dynamics in Litopenaeus vannamei Shrimp," *Viruses*, vol. 15, no. 9, Sep. 2023, doi: 10.3390/v15091824.

[4] H. Ariadi, D. Mahardhika, and N. Puspitasari, "COMPARISON OF ECOLOGICAL AND FINANCIAL FEASIBILITY PATTERNS IN VANAME (L. vannamei) CULTIVATION ACTIVITIES," *Fish Scientiae*, vol. 11, no. 2, Dec. 2021.

[5] A. Prayogi, A. Azizah, and I. Pekalongan, "PENGEMBANGAN BUDIDAYA UDANG VANAME SEBAGAI UPAYA PEMBERDAYAAN MASYARAKAT DI DESA SEMUT, WONOKERTO, PEKALONGAN," 2022.

[6] C. Zhang *et al.*, "Identification and Functional Analysis of a Key Gene in the CHH Gene Family for Glucose Metabolism in the Pacific White Shrimp Litopenaeus vannamei," *Int. J. Mol. Sci.*, vol. 26, no. 10, May 2025, doi: 10.3390/ijms26104612.

[7] Y. Sun, S. Zhang, W. Feng, Y. Zhang, T. Han, and J. Wang, "Impact of Dietary Carbohydrate Levels on Growth Performance, Feed Efficiency, and Immune Response in Litopenaeus vannamei Cultured in Biofloc Systems," *Metabolites*, vol. 15, no. 6, Jun. 2025, doi: 10.3390/metabo15060409.

[8] Y. Duan, G. Zhong, Y. Nan, Y. Yang, M. Xiao, and H. Li, "Effects of Nitrite Stress on the Antioxidant, Immunity, Energy Metabolism, and Microbial Community Status in the Intestine of Litopenaeus vannamei," *Antioxidants*, vol. 13, no. 11, Nov. 2024, doi: 10.3390/antiox13111318.

e-ISSN : 2356-2579 | p-ISSN : 1412-2693, DOI : 10.62411/tc.v25i3.16203

[9] Q. Ma *et al.*, "Effects of a phytobiotic-based additive on the growth, hepatopancreas health, intestinal microbiota, and Vibrio parahaemolyticus resistance of Pacific white shrimp, Litopenaeus vannamei," *Front. Immunol.*, vol. 15, 2024, doi: 10.3389/fimmu.2024.1368444.

[10] G. Reyes *et al.*, "Microbiome of Penaeus vannamei Larvae and Potential Biomarkers Associated With High and Low Survival in Shrimp Hatchery Tanks Affected by Acute Hepatopancreatic Necrosis Disease," *Front. Microbiol.*, vol. 13, May 2022, doi: 10.3389/fmicb.2022.838640.

[11] M. Su, X. Zhang, J. Yuan, X. Zhang, and F. Li, "The Role of Insulin-like Peptide in Maintaining Hemolymph Glucose Homeostasis in the Pacific White Shrimp Litopenaeus vannamei," *Int. J. Mol. Sci.*, vol. 23, no. 6, Mar. 2022, doi: 10.3390/ijms23063268.

[12] F. Chang *et al.*, "Physiological and muscle tissue responses in Litopenaeus vannamei under hypoxic stress via iTRAQ," *Front. Physiol.*, vol. 13, Aug. 2022, doi: 10.3389/fphys.2022.979472.

[13] Y. Zhang *et al.*, "Differential Toxicity Responses between Hepatopancreas and Gills in Litopenaeus vannamei under Chronic Ammonia-N Exposure," *Animals*, vol. 13, no. 24, Dec. 2023, doi: 10.3390/ani13243799.

[14] A. Mulyadin, N. Rahmawaty Arma, A. Nasir, I. Dewi, and P. Pertanian Negeri Pangkajene Kepulauan, "Sosialisasi Upaya Pengendalian Penyakit Udang Vaname di Desa Maroneng, Kabupaten Pinrang," 2025. [Online]. Available: https://jurnal.bsi.ac.id/index.php/abdimas

[15] M. F. Nazarudin *et al.*, "Optimizing Shrimp Culture Through Environmental Monitoring: Effects of Water Quality and Metal Ion Profile on Whiteleg Shrimp (Litopenaeus vannamei) Performance in a Semi-Intensive Culture Pond," *Water (Switzerland)*, vol. 17, no. 19, Oct. 2025, doi: 10.3390/w17192818.

[16] B. Ansani Takwin *et al.*, "Respon Pertumbuhan Udang Vaname (Litopenaeus vannamei) terhadap Pakan Ekstrak Daun Jarak Pagar (Jatropha curcas) dengan Dosis Berbeda," *BIOTECHNOLOGY AND CONSERVATION*, vol. 1, no. 3, 2025, doi: 10.29303/jmbc.v1i3.7399.

[17] Rijal, Megawati, and Yusuf Muhammad Yusri, "Pengaruh Padat Tebar Benur terhadap Pendapatan pada Usaha Budidaya Udang Vaname (Litopenaeus Vannamei)," *Zoologi : Jurnal Ilmu Peternakan, Ilmu Perikanan, Ilmu Kedokteran Hewan*, vol. 3, no. 2, pp. 13–25, Jul. 2025, doi: 10.62951/zoologi.v3i2.195.

[18] R. I. Firdaus, W. H. Sugiharto, and M. I. Ghozali, "Implementasi Convolutional Neural Network Dalam Sistem Otomatis Pemilahan Sampah Infeksius Berbasis Citra Digital," *SisInfo : Jurnal Sistem Informasi dan Informatika*, vol. 7, no. 1, pp. 2655–8611, Feb. 2025.

[19] R. Novriadi, T. H. Prihadi, H. S. D. Saragih, J. Kesselring, and B. Standen, "Well-defined multispecies probiotic and enzyme combination outperforms traditional fermented probiotic applications in an intensive Pacific white shrimp, Litopenaeus vannamei (Boone, 1931), culture system," *J. World Aquac. Soc.*, vol. 54, no. 1, pp. 156–166, Feb. 2023, doi: 10.1111/jwas.12935.

[20] E. Bendra Agustina, Y. Lestiyanti, Y. Ihza Tachriri, N. Ulfiya, and P. Studi Fisika, "Analisis Pengaruh Limbah Cair terhadap Kualitas Air Sungai di Kota Pekalongan," *Media Cetak*, vol. 4, no. 2, pp. 230–239, Apr. 2025, doi: 10.55123/insologi.v4i2.5117.

[21] Y. I. Tachriri *et al.*, "System Design of Printer Machine Using Image Classification Method Based on IoT to Optimize Production Output," *SENTRI: Jurnal Riset Ilmiah*, vol. 5, no. 3, pp. 2963–1130, Mar. 2026, doi: 10.55681/sentri.v5i3.5986.

[22] T. Aung, R. Vanichviriyakit, K. Chayantrakom, S. Amornsamankul, and P. Huabsomboon, "CNN-Based Identification of Pathogens of Concern in Shrimp," *Animals*, vol. 15, no. 21, p. 3194, Nov. 2025, doi: 10.3390/ani15213194.

[23] K. Ain, O. N. Rahma, A. P. Putra, N. Syavinas, D. Darmawan, and H. Sohal, "Bone fracture detection using electrical impedance tomography based on STEMlab Red Pitaya," *Indonesian Journal of Electrical Engineering and Computer Science*, vol. 32, no. 1, pp. 150–159, Oct. 2025, doi: 10.11591/ijeecs.v32.i1.pp150-159.

[24] R. Julianto, A. Mujtahid Anas, and Mitrayana, "Characterization of photoacoustic tomography based on 450 nm visible light and its application for detection of formalin fish meat," *J. Phys. Conf. Ser.*, vol. 2498, no. 1, p. 012015, May 2023, doi: 10.1088/1742-6596/2498/1/012015.

[25] J. C. K. Tan and M. T. Coroneo, "Diagnostic interpretation of corneal tomography using a multimodal large language model (ChatGPT)," *Am. J. Ophthalmol. Case Rep.*, vol. 40, Dec. 2025, doi: 10.1016/j.ajoc.2025.102441.

[26] Elvinda Bendra Agustina, Dian Arif Rachman, Yusril Ihza Tachriri, Jessika Artamevira, and Khusfiatul Kholisah, "Rancang Bangun Smart Feeder Terintegrasi Monitoring Kualitas Air

e-ISSN : 2356-2579 | p-ISSN : 1412-2693, DOI : 10.62411/tc.v25i3.16203

Bertenaga Surya Berbasis IoT pada Budidaya Perikanan," *INSOLOGI: Jurnal Sains dan Teknologi*, vol. 4, no. 6, pp. 1701–1711, Dec. 2025, doi: 10.55123/insologi.v4i6.6658.

[27] S. E. Catsamas, G. R. Myers, and A. M. Kingston, "Physically interpretable dynamic tomography via a first-principles model," *Tomography of Materials and Structures*, vol. 9, p. 100077, Sep. 2025, doi: 10.1016/j.tmater.2025.100077.

[28] Y. I. Tachriri, E. B. Agustina, D. A. Rachman, A. W. Sari, I. Karimah, and J. Artamevira, "Detection and Analysis of Batik Waste Using Image Processing Methods in Pekalongan Regency," *Techno.Com*, vol. 24, no. 4, pp. 1262–1279, Nov. 2025, doi: 10.62411/tc.v24i4.14849.

[29] B. Correia, O. Pacheco, R. J. M. Rocha, and P. L. Correia, "Image-Based Shrimp Aquaculture Monitoring," *Sensors*, vol. 25, no. 1, Jan. 2025, doi: 10.3390/s25010248.

[30] M. Jawaid, M. Märtens, and T. J. Chin, "Event-RGB fusion for spacecraft pose estimation under harsh lighting," *Aerosp. Sci. Technol.*, vol. 168, Jan. 2026, doi: 10.1016/j.ast.2025.111039.

[31] A. Windra Sari, R. Widyaningrum, and A. Setiawan, "System Design of a Non-invasive Photoacoustic Imaging System for Imaging Teeth," *Wahana Fisika*, no. 2, p. 78, Dec. 2025, doi: 10.17509/wafi.v10i2.90699.

e-ISSN : 2356-2579 | p-ISSN : 1412-2693, DOI : 10.62411/tc.v25i3.16203